Available online at www.sciencedirect.com

ScienceDirect

Energy Procedia 159 (2019) 28–33

Energy Procedia

www.elsevier.com/locate/procedia

Applied Energy Symposium and Forum, Renewable Energy Integration with Mini/Microgrids, REM 2018, 29–30 September 2018, Rhodes, Greece

CFD Investigation of the Open Center on the Performance of a Tidal Current Turbine

Silvio Barbarelli[a], Teresa Castiglione[a]*, Giacomo Lo Zupone[b], Sergio Bova[a] and Jinyue Yan[c]

[a]*Department of Mechanical, Energy and Management Engineering, University of Calabria, Ponte Bucci, Cubo 44C, Rende 87036, Italy*
[b]*Institute of New Energy and Low-carbon Technology, Sichuan University, Chengdu, PRC*
[c]*The Royal Institute of Technology (KTH), Division of Energy Processes, Stockholm, Sweden*

Abstract

In the present paper, a revision of the layout of an innovative open center self-balancing tidal turbine is presented. Initially, the design was characterized by a central deflector, responsible for the machine equilibrium, hosted in the central part of the machine; the presence of this device, however, affected the size of the opening. Moreover, the turbine was conceived as connected to a steel rope subject to tensile stress. These peculiarities brought some critical issues due to the excessive length of the rope and to the size of the deflector, which constrained the diameters ratio. The new design involves the possibility of reducing the anchoring line length by substituting the rope with a series of tubular elements connected by alternate heavy and light nodes. The heavy nodes can gather the anchoring line when the tides stops acting. Moreover, the light nodes are floating deflectors, which develop the same action of the central deflector, whose size, in this configuration, does not affect the equilibrium. In the new machine configuration, the main deflector is located out of the center so that it can counterbalance the torque exerted by the rotor during its rotation. Finally, by means of CFD simulations, some criteria for assessing the best diameter ratio are defined.

Keywords: tidal current; marine turbine; power coefficient; CFD analysis;

* Corresponding author. Tel.: +39-0984-494162;
E-mail address: teresa.castiglione@unical.it

1876-6102
10.1016/j.egypro.2018.12.013

1. Introduction

Tidal energy has a great potential to provide large amounts of electricity and to mitigate greenhouse gas emissions. Recent estimates of the exploitable marine current power are 75 GW in the world and about 11 GW in Europe [2]. Its exploitation is especially suitable in islands located rather near to the shore, where tidal currents can reach interesting values of velocity and where the current direction is parallel to the coast owing to the bottleneck effect, for applications in isolated microgrids [1]. Technologies, developed *ad-hoc* to exploit these currents, can provide a guaranteed amount of energy, which is perfectly predictable and can be, therefore, integrated within storage and backup planning.

The technology for extracting energy from marine currents has reached very satisfactory levels is terms of performance and reliability, as it takes advantage of the modern horizontal wind turbines experience, whose design approach is based on the blade element momentum theory (BEMT) [3].

A more recent approach in designing marine turbines, makes use of Computational Fluid Dynamics (CFD), which is widely spreading, thanks to the development of numerical methods and to increasing computer resources. CFD and BEMT calculations provide quite similar results in terms of global turbine performance but the CFD approach offers more detailed flow features around the turbine and a more accurate performance estimation.

The different design procedures are jointly used today with the goal of enhancing the performance of marine turbines [4, 5]. Among the various solutions, turbines with a central hole have been proposed, which are expected to have several advantages. However, no studies were found in the literature, which demonstrate the expected performance enhancement of this configuration with respect to the conventional tidal turbines.

In the current paper, the authors propose a significant revision of a non-conventional tidal current turbine design, characterized by an open center, involving the substitution of the rope connecting the turbine to the shore with an anchoring line constituted of tubular elements linked by alternate heavy and light nodes. Another modification regards the displacement of a deflector, responsible for the machine equilibrium [6], from the central zone in an offset position. This last feature makes the machine free from any internal/external diameters ratio constraints and the open center dimensions can be properly chosen. This last aspect, in particular, is investigated herein, the related hydrodynamic effects are analyzed and the detection of optimal dimensions of the open-center, which maximize the power/weight ratio is sought.

2. Machine Configuration

The basic idea of the machine design involves the elimination of expensive and complex structures, supports or foundations. To this aim, in a preliminary configuration, the machine design provides the use of a simple rope, which connects the machine to the coast; the rope is subject to a tensile stress and keeps the machine in an equilibrium position, which does not change during operation. The fundamental elements of the machine are: the rotor, the stator with built in a permanent magnet generator and a central deflector. The force produced by the rotor during its rotation (T) combines with the lift (L_{defl}) acting on the central deflector so that the resultant force (R) stretches the rope creating the positioning angle β, invariable during the operations, as shown in Fig.1 [6,7].

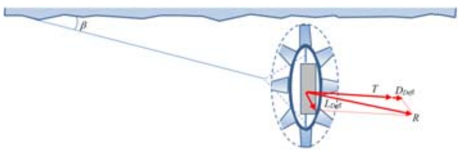

Fig. 1. Machine configuration and working principle.

This first turbine configuration, however, is very hard to manage and presents several critical issues. These regard: a) excessive length of the rope because of the low values of the beta angle needed for guaranteeing low diameters ratios (D_i/D_e) and then high rotors area; b) high size of the cross-section of the rope when the dimensions of the turbine increase and, consequently, the resultant force, R, stretching the rope increases. With the aim to simplify the turbine operations, two significant modifications have been made: the rope is substituted with a series of heavy and light nodes connected by tubular elements and an offset deflector is introduced.

2.1. Substitution of the rope with tubular elements

The scheme of the new configuration is illustrated in Fig. 2a. The anchoring line is made up of heavy and light nodes connected by tubular elements, the light nodes being floating deflectors able to receive a lift thrust from the sea currents. The forces acting on these floating deflectors are lift (L_{Fl}) and drag (D_{Fl}). When the turbine rotates, they produce a considerably high thrust T, owing to the rate of change of the axial momentum [7].

The above-described forces can be decomposed into components acting along the anchoring line, and into components acting perpendicularly to it. The latter cancel each other out, while the resultant effect of the other forces will stretch the line of the turbine creating a positioning angle β, different from the original configuration, which does not change during operation.

2.2. Implementation of an offset deflector

The new configuration is highlighted in Fig.2b. The deflector is in an offset position and allows the lift forces acting on it (L_{Defl}) to create a clockwise torque ($T= L_{defl}\ b$), which is equal and opposite of that due to the counter clockwise rotation of the rotor. In this way, roll stability control is guaranteed.

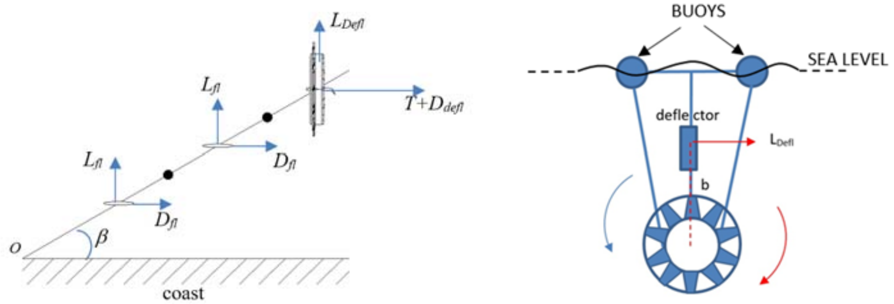

a) **b)**

Fig. 2 a)Working principle of the new anchoring system–top view; b) Scheme of the new turbine configuration

The sizing of the deflector is determined both bythe turbine geometrical parameters, like the rotor area and the arm, b, of the deflector, and by fluid dynamic parameters, like the deflector lift coefficient L_{Defl} and the turbine power coefficient, C_p. The main advantages of this new configuration are related to the possibility of recovering useful space and reducing the central hole diameter to values which guarantee the best performance with respect to the rotor area. In fact, a large turbine hole implies high values of the power coefficient in spite of a low rotor area, hence low extracted power; on the contrary, a small hole guarantees a large rotor area but a lower C_p coefficient.

The objective of the present paper is to clarify the effects of the central hole size. Three machine configurations are considered: traditional full-length blade turbine; open-center turbine with the central hole covering an area of about 65% of the total disc area; open-center turbine with the central hole covering an area of about 25% of the total disc area. A summary of the geometrical parameters for the current study is presented in Table 1. Owing to the occurrence of blades overlapping, the number of blades in the full-length configuration is limited to six, while, for the open center configurations, twelve blades are adopted. The study is carried out by means of CFD simulations.

3. CFD Analysis

Numerical simulations are carried out with the commercial code FLUENT. The use of a rotating reference frame allows the problem to be treated as steady; in particular, the Multiple Reference Frame (MRF) approach is adopted to model the rotating components. The use of this approach requires the subdivision of the computational domain into stationary and rotating zones, which are separated by interfaces where appropriate transformations of the velocity vector and velocity gradients are performed to determine fluxes of mass, momentum and other scalars.

Table 1. Machine Configurations.

Config.	Number of blades	Di/De	Central hole area (% of total disc area)	Geometry
a) full length blade	6	0.2	0	
b) large open center	12	0.8	65	
c) small open-center	12	0.5	25	

The whole computational domain is composed of two blocks, which include the rotor subdomain and the background block. Between the subdomains, non-matching interfaces are defined. The computational domain has a length of 9D and a radius of 3D, where D represents the turbine diameter. At the inlet, a constant value of water velocity is applied and a no-slip condition is enforced on the turbine blade surfaces. The use of a periodic boundary condition on the domain sides allows the reduction of the computational effort. Unstructured mesh with tetrahedral cells is used in order to overcome the difficulty of generating the mesh around complex geometries. Grid refinement occurs in proximity of the blade surface near the leading edge, trailing edge and blade tip.

4. Results and Discussion

The performance of each modelled case is characterized through the power coefficient, C_p, and the Power/Weight ratio. The C_p is defined as:

$$C_p = \frac{z \cdot M_z \cdot \frac{2\pi N}{60}}{\frac{1}{2} \cdot \rho \cdot V_0^3 \cdot \frac{\pi}{4}\left(D_e^2 - D_i^2\right)} \qquad (1)$$

It is the ratio between the extracted power and the maximum extractable power. The reference area that must be considered in this case is the rotor swept area, not the total frontal area of the device, so that, while for the full-length blade there is no difference among these two reference areas, on the contrary, these are substantially different for the open-center configurations.

Current simulations are carried out for an external machine diameter of about D_e*=1.12m* and considering a undisturbed stream velocity v_0*=3m/s.*

For configuration *a)* (see Tab. 1), corresponding to the full-length blade machine, the extracted power amounts to 5.2kW. The maximum extractable power is about 13.8 kW; consequently, the C_P is about 0.38. The flow field obtained through the CFD analysis is depicted in Fig.3a, which shows the streamlines along the computational domain. The opening of the stream-tube and the helical vortex behind the blades are well visible in proximity of the machine.

For configuration *b),* characterized by a large open center, the extracted power is about 2.6kW, which, compared to the maximum allowable power of about 4.7 kW, gives a power coefficient C_p=0.54. The power coefficient obtained in this case is higher than the one of the full-length blade. This can be explained by making a comparison of the flow field behind the rotor in both cases. In the case of the full-length blade, the pitch of the helical vortex in the inner region, close to the center of the machine, is lower than the outer region vortex (Fig. 3a) (high vorticity); the tangential component of velocity, in the central zone, is predominant with respect to the axial component. Consequently, the friction effects increase, especially in proximity of the inner region where the energy losses increase. On the contrary, when the inner part of the blade is removed, the wake is characterized by a vortex with a higher pitch angle (low vorticity) than the full-length blade (Fig.3b). Furthermore, the presence of the undisturbed flow filed in the open center tends to drag the fluid fillets and to further increase the helical vortex pitch. In this case, the axial component is predominant with respect to the tangential one; hence the power losses reduce.

A further analysis is carried out for configuration *c)*, having an intermediate open-center diameter between cases *a)* and *b)*. The extracted power is about 4.1kW and a power coefficient of about 0.42 is obtained. This value is intermediate between the full-length (C_P=0.38) and the short-length blade (C_P=0.54). This behavior is consistent with the expectations; in fact, the longer blade height, with respect to case *b)*, reduces the central hole diameter, increases the portion of the flow field characterized by the swirl and reduces, therefore, the power coefficient.

In summary, for a fixed machine external diameter, by reducing the blade height and increasing the area of the central hole, the power coefficient increases. This is due to the increase of the flow rotation in that portion of blade closer to the machine center, which increases the energy losses.

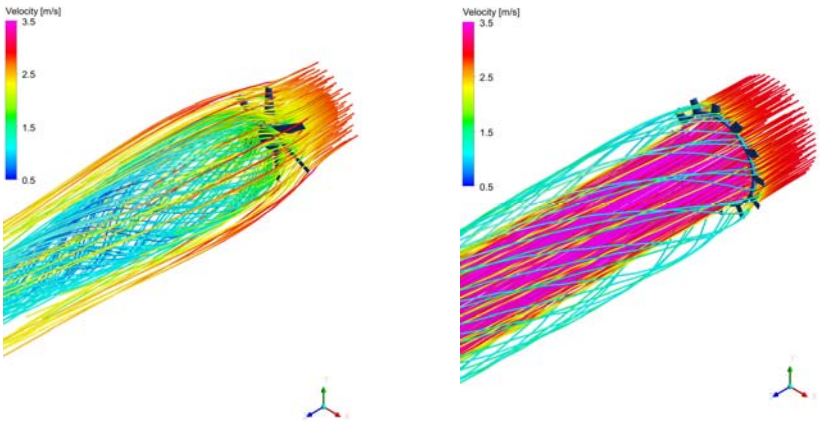

a) **b)**

Fig. 3 Streamlines for machine configurations a) and b)

In spite of the increase of the power coefficient, the maximum extracted power, however, is lower owing to the reduction in the exploitable disc area. The power/weight ratio was estimated for each configuration, by considering that the turbine is made in aluminum. The results of the CFD analysis for all the proposed geometries are summarized in Table 2 and are plotted in Fig.4 and these show that the configuration with the shorter blade presents the advantages to increase the machine C_p, allows reducing considerably the machine weight. However, the presence of a central hole implies a lower extracted power than a traditional full-length blade machine having the same diameter.

5. Summary and Conclusions

A new layout of an innovative open-centre self-balancing tidal turbine, suitable even for applications in isolated microgrids, was presented. A hydrodynamic analysis was performed in order to assess the performance of the new concept tidal turbine and to evaluate the effects due to the presence of the open centre. Numerical simulations were carried out for a traditional full-length blade turbine, a rotor with a large open centre and a rotor with a reduced open centre, for a fixed external diameter. The results demonstrated that the presence of a central hole increases the power/weight ratio; the extracted power, on the contrary,

Table 2. Summary of the CFD results for the three machine configurations

Config.	C_P	Power *(kW)*	Power/Weight *(kW/kg)*
a) full-length blade	0.38	5.2	0.3
b) large open center	0.54	2.6	0.9
c) small open center	0.42	4.1	0.4

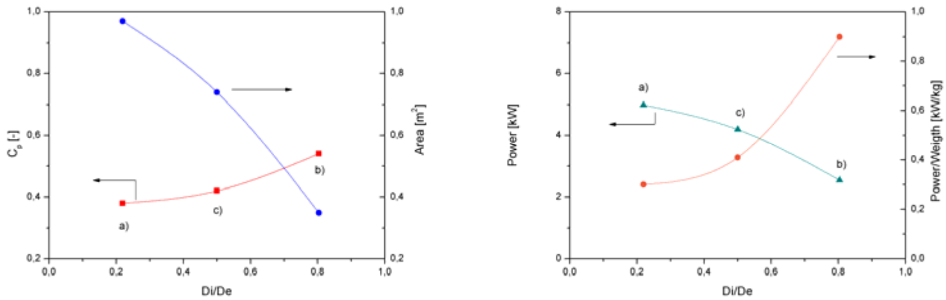

a) b)

Fig. 4 a) Power coefficient and disc surface area and b) Power and Power/Weight ratio for the three machine configurations a), b) and c).

diminishes owing to a reduced swept area, which has a greater effect than the increase in power coefficient. The overall convenience in defining the central hole dimension must be evaluated by adopting other parameters, like the LCOE, the payback time and the incidence of the material cost with respect to the overall costs.

References

[1] Zia MF, Elbouchikhi E, Benbouzid M. Microgrids energy management systems: A critical review on methods, solutions, and prospects. Appl Energy. 2018; 222:1033-55. Available from: https://doi.org/10.1016/j.apenergy.2018.04.103.

[2] Boye H, Caquot E, Clemet P et al. Rapport de la mission d’etude sur les énergies marines renouvables. Available from: www.developpement-durable.gouv.fr/IMG/pdf/RAPPORT_ENERGIES_MARINES_2013.pdf.

[3] Burton T, Sharpe D, Jenkins N, Bossanyi E. Wind energy handbook. Wiley, 2000.

[4] Rourke FO, Boyle F, Reynolds A. Tidal Energy update-2009. Appl Energy. 2010; 87:398-409. Available from: https://doi.org/10.1016/j.apenergy.2009.08.014

[5] Zhou Z, Benbouzid M., Charpentier JF, Scuiller F. Developments in large marine current turbine technologies- A review. Renew Sustain Energy Rev. 2017; 71:852-858. Available from: https://doi.org/10.1016/j.rser.2016.12.113.

[6] Barbarelli S, Amelio M, Castiglione T, Florio G, Scornaienchi NM, Lo Zupone G, Cutrupi A. Analysis of the equilibrium conditions of a double rotor turbine prototype designed for the exploitation of the tidal currents. Energy Convers Manag. 2014; 87:1124–33. Available from: https://doi.org/10.1016/j.enconman.2014.03.046.

[7] Barbarelli S, Florio G, Lo Zupone G, Scornaienchi NM. First techno-economic evaluation of array configuration of self-balancing tidal kinetic turbines. Renew Energy. 2018; 129:183-200. Available from: https://doi.org/10.1016/j.renene.2018.06.007.